THE JOURNAL OF PHYSICAL CHEMISTRY C

Article

pubs.acs.org/JPCC

Origin of Charge Separation at Organic Photovoltaic Heterojunctions: A Mesoscale Quantum Mechanical View

Mosè Casalegno,[†] Raffaele Pastore,[‡] Julien Idé,[§] Riccardo Po,[∥] and Guido Raos*[,†]

[†]Dipartimento di Chimica, Materiali e Ing. Chimica "G. Natta", Politecnico di Milano, Via L. Mancinelli 7, Milano 20131, Italy

[‡]CNR-SPIN, Via Cintia, Napoli 80126, Italy

[§]Laboratory for Chemistry of Novel Materials, University of Mons, Mons B7000, Belgium

[∥]Research Center for Renewable Energies & Environmental R&D, Eni SpA, Via G. Fauser 4, Novara 28100, Italy

Supporting Information

ABSTRACT: The high efficiency of charge generation within organic photovoltaic blends apparently contrasts with the strong "classical" attraction between newly formed electron−hole pairs. Several factors have been identified as possible facilitators of charge dissociation, such as quantum mechanical coherence and delocalization, structural and energetic disorder, built-in electric fields, and nanoscale intermixing of the donor and acceptor components of the blends. Our mesoscale quantum-chemical model allows an unbiased assessment of their relative importance, through excited-state calculations on systems containing thousands of donor and acceptor sites. The results on several model heterojunctions confirm that the classical model severely overestimates the binding energy of the electron−hole pairs, produced by vertical excitation from the electronic ground state. Using physically sensible parameters for the individual materials, we find that the quantum mechanical energy difference between the lowest interfacial charge transfer states and the fully separated electron and hole is of the order of the thermal energy.

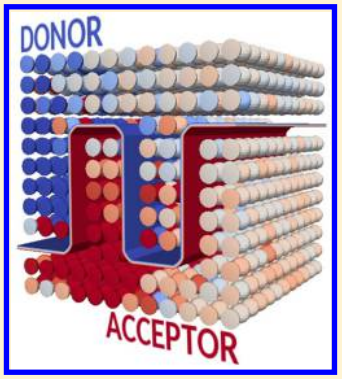

INTRODUCTION

Solar energy is by far the most abundant renewable energy source, and harvesting it to produce electricity and "solar fuels" (e.g., molecular hydrogen) seems to be the most promising route in the transition to an energetically sustainable future.[1] Silicon-based solar cells are already making a significant impact on worldwide energy production, but other photovoltaic technologies are being actively researched for the medium- and long-term. Organic photovoltaic (OPV) devices represent one of the alternatives, which could be attractive for some applications in view of the wide availability of raw materials, low production costs, and printability on mechanically flexible substrates. Their key component is a thin semiconducting active layer consisting of a blend of an electron-donor (D) and an electron-acceptor (A), which may be conjugated polymers and/or small molecules.[2−5] Today, OPV devices with 10% power conversion efficiency (PCE) have been produced by several groups,[6,7] and a record 12% PCE has been achieved with a ternary blend.[8] This has been possible thanks to a careful selection of the materials—synthetic possibilities are almost[9] limitless—and optimization of the blend structure and morphology by controlling the deposition methods and postdeposition treatments.[5,10]

As early as 2009, the group of Lee and Heeger achieved near-100% internal quantum efficiency (IQE) in "bulk heterojunction" cells having 6% PCE, based on a low-bandgap donor copolymer and a fullerene-based acceptor.[11] IQE measurements are somewhat difficult, and therefore they are not usually performed in experimental studies, but it seems likely that IQEs exceeding 90% should be achieved in all of the current state-of-the-art devices. Such high values imply that virtually every absorbed photon—the IQE is actually a function of their wavelength—is successfully converted into a negatively charged electron (transported through the A material to the cell's cathode) and a positively charged hole (transported through the D material to the cell's anode). In turn, this implies a near-100% success in each of the processes, which follow the formation of an exciton by photon absorption within either phase. According to conventional wisdom, these are the diffusion of the exciton to the D−A interface, its dissociation into a "bound" electron−hole pair or charge-transfer (CT) exciton, their separation into free charge carriers, and the migration/collection of the latter at the electrodes. This is a truly remarkable result, which apparently defies simple "classical" explanations, considering that the attractive interaction between a positive and a negative point charge at 1−2 nm distance in a medium with relative permittivity ε_r = 3−4 is 0.2−0.5 eV, which is much greater than k_BT = 0.025 eV at room temperature. This and other observations have prompted the suggestion that to understand organic photovoltaics it is essential to invoke general quantum mechanical principles of delocalization, coherence, and uncertainty,[12,13] and that it

Received: April 18, 2017
Revised: June 30, 2017
Published: July 17, 2017

DOI: 10.1021/acs.jpcc.7b03640
J. Phys. Chem. C 2017, 121, 16693−16701

might be possible to enhance the performance of OPV devices by properly harnessing them.[14]

Spectroscopic experiments have been carried out with a range of methods, allowing the characterization of the relevant species, namely excitons and polaronic charge carriers, as well as interfacial CT states, with increasing detail.[15−19] Ultrafast pump−probe experiments showed that high-energy, "hot" CT states (CT_n) tend to dissociate faster than the lower-energy ones (CT_1).[20−23] A higher rate of charge separation was linked to a higher degree of quantum mechanical coherence and delocalization and was assumed to translate into a higher overall dissociation efficiency. However, other experiments[24,25] could be interpreted more conventionally in terms of a slow (on the ps scale, in comparison with the fs scale of the previous ultrafast studies), diffusive dissociation of "classical" charge carriers. Salleo, Neher, and co-workers[26,27] have reported that "cold" CT_1 states produced by direct, weakly allowed absorption from the ground state dissociate just as efficiently (or as inefficiently, depending on the D:A combination) as the higher energy ones. On the theoretical front, charge photogeneration has been modeled by accurate excited-state or time-dependent calculations on few-molecule systems,[28−30,32] microelectrostatic[34,35] or quantum chemical calculations[36−38] on larger D:A aggregates produced by molecular dynamics simulations,[39,40] or Kinetic Monte Carlo (KMC)[41,42] and Master Equation (ME)[43] simulations at the scale of whole OPV devices. These methods have complementary strengths and weaknesses, but overall it has proved difficult to combine them to provide a general, fully satisfactory answer to the long-standing question: "Why is exciton dissociation so efficient at the interface between a conjugated polymer and an electron acceptor?"[44]

To cut a long story short, several candidates have been identified as likely "facilitators" of CT dissociation: built-in electric fields at D:A interfaces, delocalization of the excitons and of the charge carriers, high charge mobility, energetic variability and structural disorder, domain size and degree of intermixing of the D and A "phases", nonlinearity or inhomogeneity of the dielectric medium, and excess energy of the photogenerated excitons.[15−19] All of these factors seem to have some importance, but probably not equally so. Besides, some of them seem to be incompatible with each other (e.g., disorder and delocalization/mobility of the charges).

Here, we present fresh theoretical insights based on our effective two-orbital quantum chemical model,[45] which provides a "minimal" but theoretically sound description of OPV materials. It is similar in spirit to those of Troisi,[46] Bittner and Silva,[47] and Ono and Ohno,[48] but it can be applied to much larger systems. Thus, the model can provide a meaningful description of OPV operation at the mesoscale (10 nm or higher),[49] which is crucial to account for the effect of blend morphology. Unlike Bittner and Silva,[47] the present version of our model does not account for the coupled electron−nuclear dynamics, which are responsible for decoherence phenomena. On the other hand, several of the previous facilitators of CT dissociation may be readily introduced in a calculation, allowing a systematic and unbiased assessment of their relative importance, without the burden of costly atomistic molecular dynamics simulations to generate models of the D/A blends.

THE MODEL

We model portions of a photoactive layer consisting of equal number of D and A sites. Overall, there are $M = 12 \times 12 \times 12 = 1728$ sites, arranged on a simple cubic lattice with a spacing of 1.0 nm. Figure S.1 shows the structure of our six model heterojunctions. The simplest one has a planar interface between the D and A sites, while the others present some interpenetration between the phases to give a "comb" morphology (the systems have been named N*n*T*t*, according to the number n of pillars and the thickness t of the intermixing region). In general, each site may represent a whole molecule, or a π-conjugated section of a long polymer chain. There are two electrons and two orbitals per site, representing its highest occupied molecular orbital (HOMO) and lowest unoccupied molecular orbital (LUMO). This picture is similar to that adopted in KMC simulations of OPV devices, but here the electronic states are derived from a proper quantum-mechanical description, without any assumption about their localization or delocalization.

The on-site parameters of our model Hamiltonian (the HOMO and LUMO energies, as well as the Coulomb and exchange interactions among the electrons) can be chosen to reproduce exactly the energies of the main electronic states of the individual sites/molecules: lowest singlet excitation energy (SX), lowest triplet excitation energy (TX), ionization energy to form a cation (IE), and electron affinity to form an anion (EA). In our calculations, we employ a set of on-site parameters, which correspond to C_{70} for the acceptor and pentacene for the donor.[45] Taking the gas-phase experimental data as a starting point, the effect of the surrounding dielectric on the ionized states has been obtained from the Born formula for the solvation free energy of an ion. All of these energies have been collected in Table 1. Alternatively, this information about the single-molecule states could be obtained by conventional quantum chemical calculations, which can account for the surrounding dielectric by a polarizable continuum model.[50]

Table 1. Single-Molecule Energies (in eV) for the Acceptor A (C_{70}) and the Donor D (Pentacene), in the Gas Phase or within a Dielectric with $\varepsilon_r = 3.5$

	vacuum		dielectric	
energies	A	D	A	D
IE_r	7.48	6.61	6.45	5.58
EA_r	2.68	1.35	3.71	2.38
SX_r	2.44	2.28	2.44	2.28
TX_r	1.56	1.76	1.56	1.76

The intersite part of the Hamiltonian consists of a one-electron part, describing off-diagonal orbital couplings and the interaction with the positively charged cores of the other sites, and a two-electron part. The orbital couplings are assumed to be essentially random and decay exponentially with intersite distance. The intersite electron−electron and electron−core interactions are approximated by the electrostatic interaction between two spherical Gaussian charge distributions, embedded in a dielectric medium with relative permittivity $\varepsilon_r = 3.5$. As a side note, we point out that situations with degenerate or near-degenerate HOMO and LUMO levels occur frequently in fullerene-based and other materials. These could be modeled within our coarse-grained model by connecting three or four sites into "supermolecules" with D_{3h} or T_d symmetry. Two sites could be considered to be connected when their coupling is roughly 1 order of magnitude larger than that between unconnected ones. Orbital degeneracy might indeed have an

DOI: 10.1021/acs.jpcc.7b03640
J. Phys. Chem. C 2017, 121, 16693−16701

effect on charge separation and transport,[51,52] and we hope to study it in the future.

Both diagonal and off-diagonal disorder can be introduced in a controlled way, by admitting local deviations in the orbital energies and couplings. Our method allows independent, essentially unrestricted variations in their relative sizes. Here, we model them as random numbers, drawn from Gaussian distributions with standard deviations σ_w = 0.08 eV (for diagonal energetic disorder) and σ_t = 0.08 eV (for off-diagonal coupling disorder). These values are comparable to those that arise in the calculation of charge mobilities in organic semiconductors.[53−55] For a given arrangement of D and A sites, different realizations of the disorder can be generated by simply reassigning these energies and couplings, starting from a different random number seed. Typically, to extract systematic trends from our calculations, we consider 100 independent realizations of the disorder.

The ground-state energies, wave functions, and charge distributions have been obtained by self-consistent-field, restricted Hartree−Fock (HF) calculations.[56,57] The analogous excited-state properties have been obtained by configuration interaction calculations including all of the single excitations (CIS)[58] from the M occupied to the M virtual HF orbitals. CIS can be considered an excited-state extension of the HF method, as both of them neglect electron correlation effects. Note that the singly excited configurations do not contribute to the ground-state wave function, as a consequence of the variational nature of the HF solution (Brillouin's theorem). We have also evaluated the effect of nondynamical electron correlation, by comparing the results of CIS and high-level excited-state calculations (equation-of-motion coupled-cluster singles plus doubles, or EOM-CCSD).[59−61] These results will be presented at the end of the following section. All calculations have been carried out with a modified version of GAMESS-US.[62] Further details are given in the Supporting Information.

We consider the lowest energy states obtained from the CIS calculations to be close theoretical relatives of the cold CT_1 states mentioned in the Introduction.[26,27] Our states are coherent or "pure", being described by a stationary electronic wave function instead of a density matrix.[57] The current version of the model does not deal with nuclear motions, and in particular with decoherence and geometrical relaxation associated with charge transfer events.[14,63] These phenomena have been modeled at the atomistic level by calculating explicitly the time-dependence of the nuclear coordinates and electronic wave function.[30−32] Clearly, this approach cannot be directly applied to the present model. However, a time-dependent extension could be attempted by introducing a dependence of the orbital energies and couplings on some generalized intra- and intermolecular phonon coordinates.[33,47]

RESULTS AND DISCUSSION

As a preliminary step to the discussion of the electronic states at the heterojunctions, we provide some data on the pure materials. These have been obtained by HF and CIS calculations on blocks of M = 1728 D-only or A-only sites. Considering, for example, the ith realization of a donor block (D_i), the relevant energies are

$$\begin{aligned} SX(D_i) &= E_{CIS}(D_i) - E_{HF}(D_i), \\ IE(D_i) &= E_{HF}(D_i^+) - E_{HF}(D_i), \\ EA(D_i) &= E_{HF}(D_i) - E_{HF}(D_i^-) \end{aligned} \quad (1)$$

where E_{CIS} is the energy of the first excited state of the neutral system, and E_{HF} is the ground-state energy of the neutral or charged system. Table 2 gives the averages and standard deviations of these energy differences, obtained by calculation on several independent realizations of the disorder. The SX energies of A and D compare favorably with the optical band gaps of solid C_{70} (1.66 eV)[64] and pentacene (1.85 eV),[65] respectively. At the same time, these energies are substantially lower than those of the single-molecule, on-site excitations (see again Table 1). We take this as an indication that delocalization effects are significant and they are reasonably well described with our choice of the orbital coupling parameters.

Table 2. Averages and Standard Deviations of the Singlet Excitation Energies, Ionization Energies, and Electron Affinities (in eV) of the Pure Materials

material	SX	IE	EA
A	1.62 ± 0.17	5.99 ± 0.21	4.17 ± 0.15
D	1.87 ± 0.22	5.11 ± 0.19	2.85 ± 0.25

The IE and EA data in Table 2 are also interesting, as they allow us to estimate the average energy of an electron−hole pair at infinite separation. Putting the hole on the donor and the electron on the acceptor, we find

$$E_{eh}^{\infty} = IE(D) - EA(A) \quad (2)$$

The result is E_{eh}^{∞} = 0.94 ± 0.24 eV. This is roughly one-half of the energy, which could be estimated from the single-molecule data in Table 1, assuming fully localized charges (1.87 eV). This confirms the importance of delocalization effects, despite the sizable amount of disorder, which has been included in the model.

Figure 1 shows the distribution of the first and second excitation energies, calculated from 100 independent realizations of each model heterojunction. Each of them might correspond to a slight rearrangement of the molecules, resulting from a combination of intra- and intermolecular vibrations. The lowest excitation energies are of the order of 0.90 eV. The average excitation energies (continuous black lines in the figure) do not seem to depend much on the interface morphology. These band gaps are substantially lower than those of the pure phases. At the same time, the CT_1 states are within only 0.04 eV from the average E_{eh}^{∞} (dashed red lines in the figure). Note also that histograms of first and second excitations overlap strongly, each having a width of the same order of magnitude (comparable to k_BT). Thus, the second (or third) excitation energy of one system may be lower than the lowest excitation energy of another. In the following, we will concentrate on the discussion of the CT_1 states, but one should always keep in mind that there is actually a near-continuum of states above them.

We have just established that, using a resonable set of Hamiltonian parameters, the lowest interfacial excited states are within k_BT from the infinitely separated charges, contrary to the "classical" expectations. Before we look at this finding in greater depth, it is necessary to discuss its general validity. Clearly, by a proper choice of the Hamiltonian parameters, our calculations

DOI: 10.1021/acs.jpcc.7b03640
J. Phys. Chem. C 2017, 121, 16693−16701

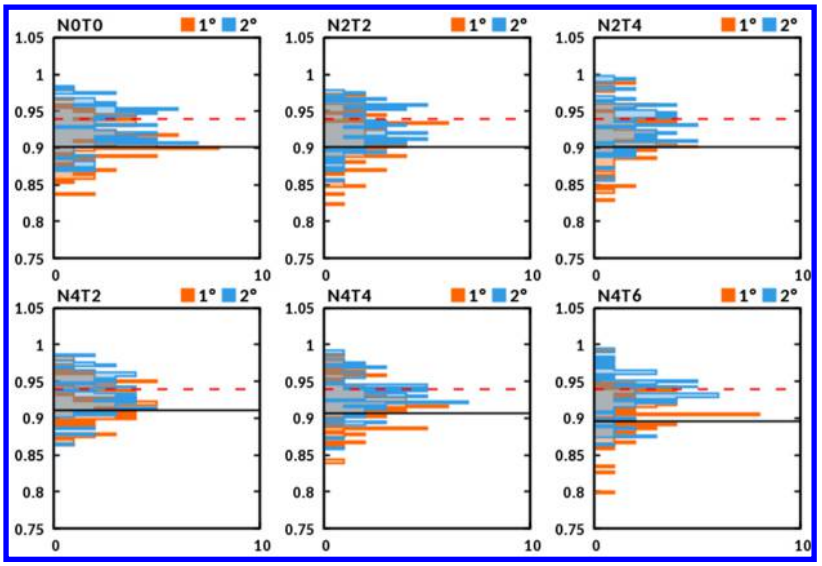

Figure 1. Distributions of the first and second excitation energies (in eV) for all of the heterojunction morphologies. The horizontal axis is the number of counts within an energy bin. The horizontal black line marks the average first excitation energy. The dashed red line marks the average energy of an electron−hole pair at infinite separation (E_{eh}^{∞}).

can be tuned to reproduce the vertical excitation and ionization energies of the donor and the acceptor. Because the model does not account for geometrical relaxation following photoexcitation, our lowest excited states are "electronically cold" but "vibrationally hot", and we are certainly overestimating the transition energies that would be measured by fluorescence spectroscopy. On the other hand, the electron−hole pairs tend to be already well separated in these excited states (see below). It is reasonable to assume that their vibrational relaxation energies are comparable to the sum of those of an electron within the A and a hole within the D. Thus, even though we are overestimating the energies of the relaxed interfacial excitons with respect to the ground state, we believe that the energies with respect to the fully separated charges should be roughly correct.

Figure 2 (upper panel) illustrates the charge distribution in the ground and the first excited states, for one realization of the flat bilayer. The sites are color-coded according to their net charges (q_k^0 for the ground state and q_k^X for the excited state, k being the site index). At first sight, the charges in the two states seem rather similar. In fact, they seem to be almost random, with several negative values on the D side and several positive ones on the A side of the interface. This randomness of the charge distribution reflects the randomness of the underlying Hamiltonian, of course.

A clear picture starts to emerge by plotting the charge difference between the states, $q_k^X - q_k^0$. Figure 2 (lower panel) shows several examples of the charge differences between the excited and the ground states, one for each instance of the model heterojunctions. The individual distributions are obviously rather different, but the overall picture is remarkably simple and consistent. We see two distinct charge pockets, which are well separated and reside entirely on the expected phases (D for positive, A for negative). Summing these charge differences, we always obtain:

$$\sum_{k\in \mathrm{D}} (q_k^X - q_k^0) = -\sum_{k\in \mathrm{A}} (q_k^X - q_k^0) = 1.00e$$

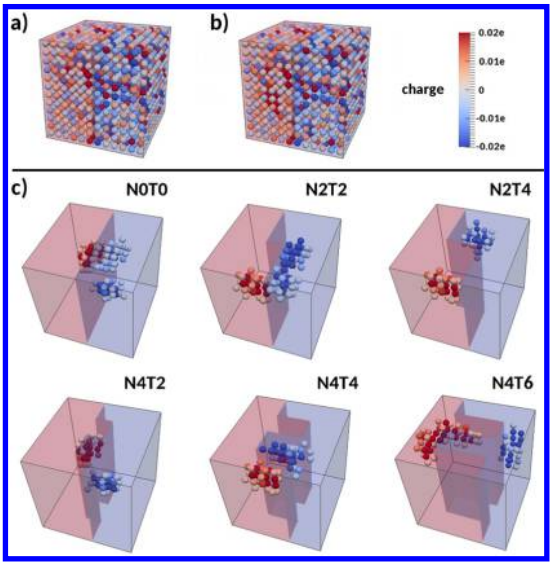

Figure 2. Upper panel: Charge distributions in one realization of the bilayer, respectively, for (a) ground state and (b) first excited singlet state. Lower panel: (c) Charge differences between the excited and ground states, for one realization of each system. The red and blue shading of the background indicates the D and A sides of the heterojunctions, respectively, whereas the coloring of the sites indicates positive (red) or negative (blue) charges. For clarity, (c) shows only the sites with a charge difference greater than 0.002e (in modulus).

so that photoexcitation produces a net transfer of one electron from the donor to the acceptor phase. These photogenerated charges appear to be delocalized over 10−20 sites, but this estimate can increase to 40−50 sites depending on the threshold adopted for their individual values. Of course, this sizable delocalization reflects the situation immediately following photoexcitation, before the nuclear motions set in to produce decoherence and further localization.

Because of the large variability in the charge distributions associated with different realizations of the Hamiltonian, it is necessary to average hundreds of them to extract further

DOI: 10.1021/acs.jpcc.7b03640
J. Phys. Chem. C 2017, 121, 16693−16701

systematic trends. Figure 3 illustrates the results for the ground states. For clarity, we present them as simple two-dimensional

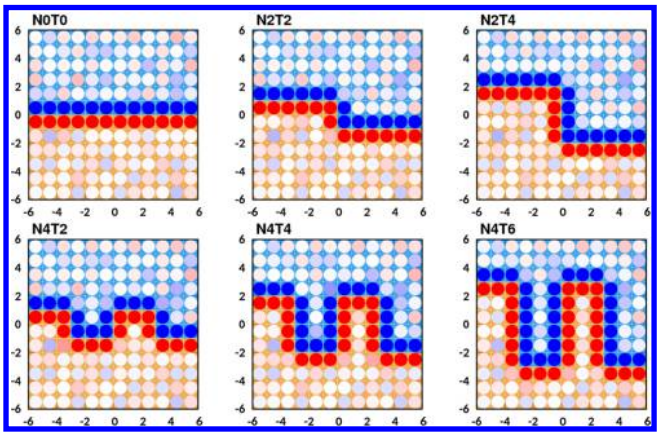

Figure 3. Two-dimensional plots of the average ground-state charge distributions, $\langle q_k^0 \rangle$. The color scale is such that saturation of the red and blue occurs when the charges exceed 0.0025*e*, in modulus.

maps. These have been extracted from the six layers at the center of the blocks, excluding those at the top and at the bottom (in the orientation of Figure 2) to minimize boundary effects. These charge density plots may also be taken to represent the result of an incoherent superposition of many quantum mechanical states, as all phase information is discarded when averaging their charge distributions. The ground-state maps demonstrate the formation of sharp, well-defined interfacial dipoles. The average charge on a site sitting at the D/A interface is 0.007*e* (in modulus). Remembering that our sites are spaced by 1 nm, this is at least comparable with the interfacial charge densities of $0.02e/\text{nm}^2$, as estimated by Bässler and Köhler[18] on the basis of the typical voltage drop at a heterojunction. The charges located on the sites away from the interface, although appreciable within a single realization of the disorder (see again Figure 2), tend to cancel each other upon averaging. Of course, the average size of the interfacial dipoles will largely depend on the energetic offset between the donor and the acceptor orbitals, and we hope to study this systematically in the future.

Figure 4 contains the analogous two-dimensional maps of the photogenerated excess charge distributions. These plots tend to be noisier than those for the ground states, but even so it is possible to draw some interesting conclusions. Naively, considering that we are looking at the lowest energy excitations, one would have expected the photogenerated charges to be "squeezed" at the interfaces by their mutual attraction. Instead, the average charge densities tend to be spread almost everywhere, except perhaps at the external boundaries of the blocks (good news, as this implies that finite-size effects are reasonably under control). In particular, there is a significant photogenerated charge density within the first 2−3 layers from the interface. The subsequent time-dependent evolution will produce some localization of the photogenerated changes. Because we cannot simulate it with the current model, we can only speculate that their average distribution will still resemble that in Figure 4. In any case, the figure highlights that a truly unbiased model of charge photogeneration should include hundreds of donor and acceptor molecules, and this is currently incompatible with a detailed atomistic description of the coupled electron−nuclear dynamics.

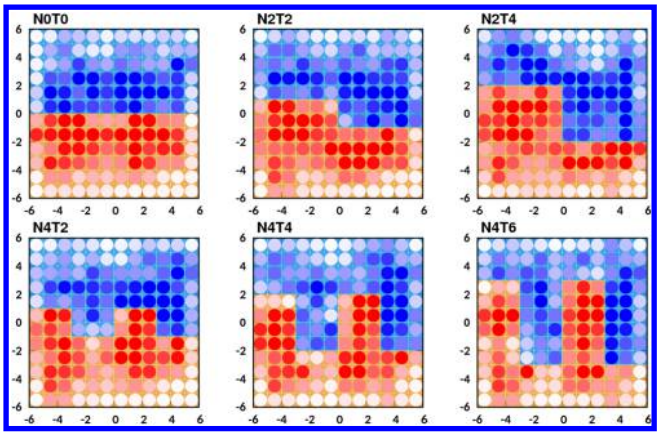

Figure 4. Two-dimensional plots of the average photogenerated excess charge distributions, $\langle q_k^X - q_k^0 \rangle$. The color scale is identical to that of Figure 3.

The electrostatic repulsion between the newly generated charges and the ground-state interfacial dipoles, or, in other words, the built-in electric field, seems to be a key factor in enhancing this electron−hole separation. Exploratory calculations with other parameter sets show that an increased conjugation (introduced in the form of higher interorbital couplings) and a lower disorder within the phases tend to produce an even greater electron−hole separation, up to a point where the photogenerated charge densities are almost zero on the D/A sites that are directly in contact. Thus, the calculations confirm the idea that both interfacial dipoles (a classical effect) and delocalization (a quantum-mechanical effect) can act as "facilitators" of charge dissociation. We also note that the orthogonality between the ground-state and the excited-state *N*-electron wave functions may represent an additional factor promoting charge separations. This is a purely quantum mechanical feature, which is built in our calculations. It has no classical analogue, and it is related to the *N*- and *v*-representability problem of an excited-state charge distribution[66] (e.g., can a "classical" charge distribution with localized electrons and holes on opposite sides of a D/A interface always be derived from an *N*-electron wave function, which is both antisymmetric and orthogonal to the ground state wave function?).

Figure 5 provides further results about the effect of interfacial morphology on the distribution of electron−hole distances. Here, the positions of the electrons and holes were identified by computing the center-of-charge of the excess photogenerated

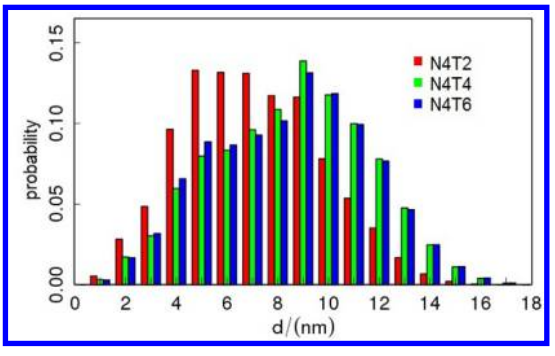

Figure 5. Distribution of the electron−hole distances for selected interfacial morphologies.

DOI: 10.1021/acs.jpcc.7b03640
J. Phys. Chem. C 2017, 121, 16693−16701

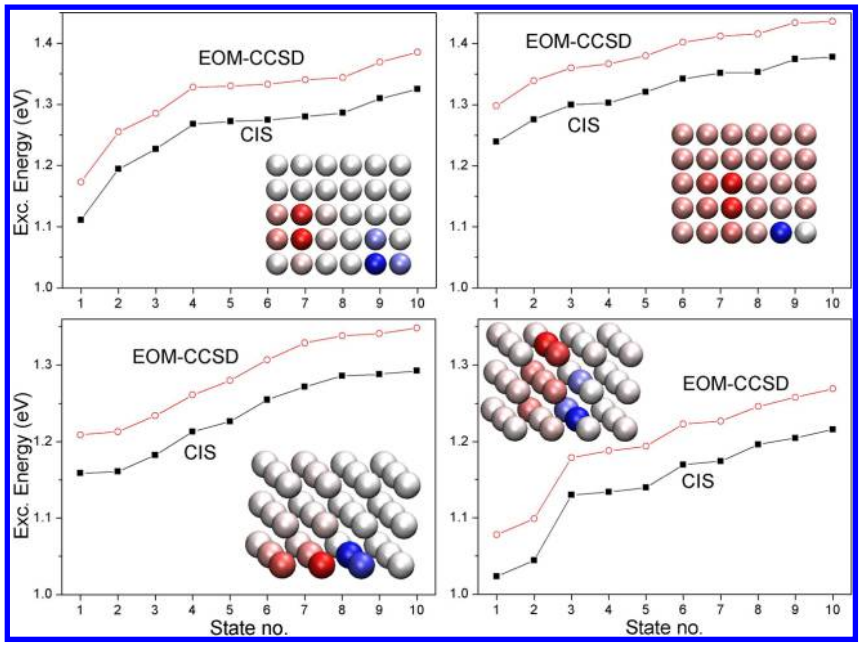

Figure 6. Comparison of CIS and EOM-CCSD calculations of the first 10 excited states, in two-dimensional (above) and three-dimensional (below) model heterojunctions. The insets show the EOM-CCSD charge distributions in the first excited states.

charges (negative and positive, respectively). The plots show that increasing the interfacial thickness from 2 (N4T2) to 4 or 6 nm (N4T4 and N4T6) should have a beneficial effect on charge separation, by shifting the distribution of electron−hole distances toward larges values. If confirmed, this observation could turn into a useful design rule for the choice of photovoltaic materials and their assembly within the active layer. In the future, we hope to corroborate it by further calculations based on more realistic off-lattice models with "arctan-like" concentrations of the donor and the acceptor.

Finally, we validate the use of the CIS method by comparing it with EOM-CCSD excited-state calculations. We have carried out benchmark calculations on two systems: a two-dimensional heterojunction consisting of 15 D and 15 A sites, and a three-dimensional heterojunction consisting of 18 D and 18 A sites. Figure 6 shows the results for two independent realizations of each system. In comparison with EOM-CCSD, CIS systematically underestimates the excitation energies by about 0.05 eV. This applies to all of the lowest excited states. As a result, one excitation spectrum is simply a shifted version of the other. Note also the significant changes in the excitation spectra, produced by simply changing the random seed for the assignment of the orbital couplings. Once more, this confirms the importance of performing extensive statistics before drawing any conclusions. The insets in Figure 6 show also the EOM-CCSD charge distribution in the lowest excited state of each system. In all cases, the CIS charge distributions (not shown) are virtually indistinguishable from them. Thus, the neglect of electron correlation in the description of the excited states of these systems appears to have a solid foundation. This is certainly good news also for those performing atomistic (ab initio or semiempirical) excited-state calculations.

■ CONCLUSIONS

We have presented the results of mesoscale quantum mechanical calculations of the lowest excited states at organic photovoltaic interfaces. Despite its relative simplicity, or perhaps thanks to it, the model allows an unbiased exploration of the effect of several possible facilitators of charge photogeneration, such as built-in or external electric fields, charge delocalization, disorder, and nanostructuring of the donor−acceptor blends. The nature of the problem requires large numbers of calculations on large systems, as it is necessary to avoid assumptions about the localization of the photogenerated charges, minimize finite-size effects, and perform adequate statistical averaging of the results. We have explored only a small fraction of the parameter space, using for example C_{70} as the only acceptor and pentacene as the only donor. Nonetheless, the results are already very encouraging, as they show that fully separated charges (electron and hole) are easily within 1−2 k_BT from the lowest excited states, in agreement with much experimental evidence but contrary to simple "classical" arguments. Delocalization emerges from our calculations as one of the key facilitators of charge dissociation. We find that a significant degree of delocalization of the excited charge transfer states (tens of molecules/sites) may occur also in the presence of some energetic and coupling disorder. On the other hand, nuclear relaxation phenomena are not included in our treatment, and as a result the real situation might be somewhere between our description and the fully localized one that is assumed in classical KMC simulations of OPV devices.

Our model is somewhat generic, as it retains a minimum of physically important features and neglects most molecular details. In this sense, it is analogous to many classical coarse-grained models of soft materials (polymers, liquid crystals, colloids, etc.), in which atomic level details are sacrificed in favor of generality, lower computational cost, and greater interpretability of the results. Considering the relative ease of achieving >90% IQEs, it seems that the photogeneration of charges is precisely a situation where a somewhat generic explanation is required. This contrasts with other aspects of the behavior of organic photovoltaic materials. Compare it, for example, with the difficulty of achieving high charge mobilities in molecular or polymeric semiconductors. This has eventually been possible thanks to a lengthy and painstaking selection of molecules and processing conditions, providing the optimal

DOI: 10.1021/acs.jpcc.7b03640
J. Phys. Chem. C 2017, 121, 16693−16701

combinations of molecular structure and supramolecular organization. Clearly, the latter is a situation where detailed molecular-level modeling is necessary to support and guide the experimental efforts. In any case, our calculations provide guidelines also for those performing more conventional, atomistic excited-state calculations at D/A heterojunctions. There is a clear need to move toward models incorporating hundreds of molecules to remove any bias about the degree of localization. This is extremely challenging, considering also the need to average over many disordered configurations, but at least our coupled-cluster calculations show that these calculations should not require the inclusion of dynamical electron correlation.

We conclude with a brief perspective on future developments. Although here we have considered idealized on-lattice models of the blend interfaces, more realistic off-lattice models are fully within our reach. It should also be interesting to examine the consequences of a polymer-like connectivity of donor or acceptor sites, to form long conjugated chains. Bittner and Silva[47] have already considered a two-dimensional system in which both the donor and the acceptor are polymeric. In their lattice model, all of the chains are parallel to the interface, and this produces low-energy charge transfer states in which the electron and hole are delocalized but "pinned" to the interface. However, the situation in a real system will be more complicated, and even a partial orientation or π-stacking of the chains in the orthogonal direction might have a strong beneficial effect on charge separation. In the longer term, the present model should be extended by incorporating electron−phonon coupling and nuclear relaxation effects, within an explicitly time-dependent picture of system. One day, with further developments along the lines of the present study, it might even become possible to simulate the operation of whole OPV devices by adding a quantum mechanical description of exciton diffusion, charge transport, and charge extraction/injection at the electrodes.

■ ASSOCIATED CONTENT

Supporting Information

The Supporting Information is available free of charge on the ACS Publications website at DOI: 10.1021/acs.jpcc.7b03640.

Detailed description of the theory and computational methods, references for the experimental gas-phase energies of pentacene and C_{70}, and illustration specifying the structure of the model heterojunctions (PDF)

■ AUTHOR INFORMATION

Corresponding Author

*E-mail: guido.raos@polimi.it.

ORCID

Raffaele Pastore: 0000-0002-8335-9961

Riccardo Po: 0000-0002-8374-195X

Guido Raos: 0000-0001-7011-4036

Notes

The authors declare no competing financial interest.

■ ACKNOWLEDGMENTS

The research of G.R. and M.C. is supported by the PRIN project "Molecular organization in organic thin films via computer simulation of their fabrication processes" (2015XJA9NT_003). The research of Ra.P. is supported by the SPIN SEED 2014 project "Charge separation and charge transport in hybrid solar cells" and the CNR−NTU joint laboratory "Amorphous materials for energy harvesting applications".

■ REFERENCES

(1) Armaroli, N.; Balzani, V. Solar electricity and solar fuels: Status and perspectives in the context of the energy transition. *Chem. - Eur. J.* **2016**, *22*, 32−57.

(2) Hains, A. W.; Liang, Z.; Woodhouse, M. A.; Gregg, B. A. Molecular semiconductors in organic photovoltaic cells. *Chem. Rev.* **2010**, *110*, 6689−6735.

(3) Po, R.; Maggini, M.; Camaioni, N. Polymer solar cells: Recent approaches and achievements. *J. Phys. Chem. C* **2010**, *114*, 695−706.

(4) Li, G.; Zhu, R.; Yang, Y. Polymer solar cells. *Nat. Photonics* **2012**, *6*, 153−161.

(5) Lu, L.; Zheng, T.; Wu, Q.; Schneider, A. M.; Zhao, D.; Yu, L. Recent advances in bulk heterojunction polymer solar cells. *Chem. Rev.* **2015**, *115*, 12666−12731.

(6) Liu, Y.; Zhao, J.; Li, Z.; Mu, C.; Ma, W.; Hu, H.; Jiang, K.; Lin, H.; Ade, H.; Yan, H. Aggregation and morphology control enables multiple cases of high-efficiency polymer solar cells. *Nat. Commun.* **2014**, *5*, 5293.

(7) Zhao, W.; Qian, D.; Zhang, S.; Li, S.; Inganäs, O.; Gao, F.; Hou, J. Fullerene-free polymer solar cells with over 11% efficiency and excellent thermal stability. *Adv. Mater.* **2016**, *28*, 4734−4739.

(8) Kumari, T.; Lee, S. M.; Kang, S.-H.; Chen, S.; Yang, C. Ternary solar cells with a mixed face-on and edge-on orientation enable an unprecedented efficiency of 12.1%. *Energy Environ. Sci.* **2017**, *10*, 258−265.

(9) Po, R.; Bianchi, G.; Carbonera, C.; Pellegrino, A. "All that glisters is not gold": An analysis of the synthetic complexity of efficient polymer donors for polymer solar cells. *Macromolecules* **2015**, *48*, 453−461.

(10) Vandewal, K.; Himmelberger, S.; Salleo, A. Structural factors that affect the performance of organic bulk heterojunction solar cells. *Macromolecules* **2013**, *46*, 6379−6387.

(11) Park, S. H.; Roy, A.; Beaupre, S.; Cho, S.; Coates, N.; Moon, J. S.; Moses, D.; Leclerc, M.; Lee, K.; Heeger, A. J. Bulk heterojunction solar cells with internal quantum efficiency approaching 100%. *Nat. Photonics* **2009**, *3*, 297−302.

(12) Kaake, L. G.; Moses, D.; Heeger, A. J. Coherence and uncertainty in nanostructured organic photovoltaics. *J. Phys. Chem. Lett.* **2013**, *4*, 2264−2268.

(13) Mukamel, S. Comment on "Coherence and uncertainty in nanostructured organic photovoltaics. *J. Phys. Chem. A* **2013**, *117*, 10563−10564.

(14) Brédas, J.-L.; Sargent, E. H.; Scholes, G. D. Photovoltaic concepts inspired by coherence effects in photosynthetic systems. *Nat. Mater.* **2016**, *16*, 35−44.

(15) Clarke, T. M.; Durrant, J. R. Charge photogeneration in organic solar cells. *Chem. Rev.* **2010**, *110*, 6736−6767.

(16) Baranovskii, S. D.; Wiemer, M.; Nenashev, A. V.; Jansson, F.; Gebhard, F. Calculating the efficiency of exciton dissociation at the interface between a conjugated polymer and an electron acceptor. *J. Phys. Chem. Lett.* **2012**, *3*, 1214−1221.

(17) Nayak, P. K.; Narasimhan, K. L.; Cahen, D. Separating charges at organic interfaces: Effects of disorder, hot states, and electric field. *J. Phys. Chem. Lett.* **2013**, *4*, 1707−1717.

(18) Bässler, H.; Köhler, A. "Hot or cold": how do charge transfer states at the donor-acceptor interface of an organic solar cell dissociate ? *Phys. Chem. Chem. Phys.* **2015**, *17*, 28451−28462.

(19) Few, S.; Frost, J. M.; Nelson, J. Models of charge pair generation in organic solar cells. *Phys. Chem. Chem. Phys.* **2015**, *17*, 2311−2325.

(20) Bakulin, A. A.; Akshay, R.; Pavelyev, V. G.; van Loosdrecht, P. H. M.; Pshenichnikov, M. S.; Niedzialek, D.; Cornil, J.; Beljonne, D.; Friend, R. H. The role of driving energy and delocalized states for

charge separation in organic semiconductors. *Science* **2012**, *335*, 1340−1344.
(21) Grancini, G.; Maiuri, M.; Fazzi, D.; Petrozza, A.; Egelhaaf, H.-J.; Brida, D.; Cerullo, G.; Lanzani, G. Hot exciton dissociation in polymer solar cells. *Nat. Mater.* **2013**, *12*, 29−33.
(22) Jailaubekov, A. E.; Willard, A. P.; Tritsch, J. R.; Chan, W.-L.; Sai, N.; Gearba, R.; Kaake, L. G.; Williams, K. J.; Leung, K.; Rossky, P. J.; Zhu, X.-Y. Hot charge-transfer excitons set the time limit for charge separation at donor/acceptor interfaces in organic photovoltaics. *Nat. Mater.* **2013**, *12*, 66−73.
(23) Jakowetz, A. C.; Böhm, M. L.; Zhang, J.; Sadhanala, A.; Huettner, S.; Bakulin, A. A.; Rao, A.; Friend, R. H. What controls the rate of ultrafast charge transfer and charge separation efficiency in organic photovoltaic blends. *J. Am. Chem. Soc.* **2016**, *138*, 11672−11679.
(24) Vithanage, D. A.; Devižis, A.; Abramavičius, V.; Infahsaeng, Y.; Abramavičius, D.; MacKenzie, R. C. I.; Keivanidis, P. E.; Yartsev, A.; Hertel, D.; Nelson, J.; Sundström, V.; Gulbinas, V. Visualizing charge separation in bulk heterojunction organic solar cells. *Nat. Commun.* **2013**, *4*, 2334.
(25) Matheson, A. B.; Pearson, S. J.; Ruseckas, A.; Samuel, I. D. W. Charge pair dissociation and recombination dynamics in a P3HT-$PC_{60}BM$ bulk heterojunction. *J. Phys. Chem. Lett.* **2013**, *4*, 4166−4171.
(26) Vandewal, K.; Albrecht, S.; Hoke, E. T.; Graham, K. R.; Widmer, J.; Douglas, J. D.; Schubert, M.; Mateker, W. R.; Bloking, J. T.; Burkhard, G. F.; Sellinger, A.; Fréchet, J. M. J.; Amassian, A.; Riede, M. K.; McGehee, M. D.; Neher, D.; Salleo, A. Efficient charge generation by relaxed charge-transfer states at organic interfaces. *Nat. Mater.* **2014**, *13*, 63−68.
(27) Albrecht, S.; Vandewal, K.; Tumbleston, J. R.; Fischer, F. S. U.; Douglas, J. D.; Fréchet, J. M. J.; Ludwigs, S.; Ade, H.; Salleo, A.; Neher, D. On the efficiency of charge transfer state splitting in polymer:-fullerene solar cells. *Adv. Mater.* **2014**, *26*, 2533−2539.
(28) Few, S.; Frost, J. M.; Kirkpatrick, J.; Nelson, J. Influence of chemical structure on the charge transfer state spectrum of a polymer:fullerene complex. *J. Phys. Chem. C* **2014**, *118*, 8253−8261.
(29) Baumeier, B.; Rohlfing, M.; Andrienko, D. Electronic excitations in push-pull oligomers and their complexes with fullerene from many-body Green's functions theory with polarizable embedding. *J. Chem. Theory Comput.* **2014**, *10*, 3104−3110.
(30) Akimov, A. V.; Prezhdo, O. V. Nonadiabatic dynamics of charge transfer and singlet fission at the pentacene/C60 interface. *J. Am. Chem. Soc.* **2014**, *136*, 1599−1608.
(31) Huix-Rotllant, M.; Tamura, H.; Burghardt, I. Concurrent effects of delocalization and internal conversion tune charge separation at regioregular polythiophene-fullerene heterojunctions. *J. Phys. Chem. Lett.* **2015**, *6*, 1702−1708.
(32) Akimov, A. V. Nonadiabatic molecular dynamics with tight-binding fragment molecular orbitals. *J. Chem. Theory Comput.* **2016**, *12*, 5719−5736.
(33) Zhugayevych, A.; Tretiak, S. Theoretical description of structural and electronic properties of organic photovoltaic materials. *Annu. Rev. Phys. Chem.* **2015**, *66*, 305−330.
(34) Verlaak, S.; Beljonne, D.; Cheyns, D.; Rolin, C.; Linares, M.; Castet, F.; Cornil, J.; Heremans, P. Electronic structure and geminate pair energetics at organic-organic interfaces: The case of pentacene/C_{60} heterojunctions. *Adv. Funct. Mater.* **2009**, *19*, 3809−3814.
(35) Poelking, C.; Tietze, M.; Elschner, C.; Olthof, S.; Hertel, D.; Baumeier, B.; Würthner, F.; Meerholz, K.; Leo, K.; Andrienko, D. Impact of mesoscale order on open-circuit voltage in organic solar cells. *Nat. Mater.* **2014**, *14*, 434−439.
(36) Yost, S. R.; van Voorhis, T. Electrostatic effects at organic semiconductor interfaces: A mechanism for "cold" exciton breakup. *J. Phys. Chem. C* **2013**, *117*, 5617−5625.
(37) Savoie, B. M.; Rao, A.; Bakulin, A. A.; Gelinas, S.; Movaghar, B.; Friend, R. H.; Marks, T. J.; Ratner, M. A. Unequal partnership: Asymmetric roles of polymeric donor and fullerene acceptor in generating free charge. *J. Am. Chem. Soc.* **2014**, *136*, 2876−2884.
(38) D'Avino, G.; Muccioli, L.; Olivier, Y.; Beljonne, D. Charge separation and recombination at polymer-fullerene heterojunctions: Delocalization and hybridization effects. *J. Phys. Chem. Lett.* **2016**, *7*, 536−540.
(39) Lee, C.-K.; Pao, C.-W.; Chu, C.-W. Multiscale molecular simulations of the nanoscale morphologies of P3HT:PCBM blends for bulk heterojunction organic photovoltaic cells. *Energy Environ. Sci.* **2011**, *4*, 4124−4132.
(40) Idé, J.; Méreau, R.; Ducasse, L.; Castet, F.; Bock, H.; Olivier, Y.; Cornil, J.; Beljonne, D.; D'Avino, G.; Roscioni, O. M.; Muccioli, L.; Zannoni, C. Charge dissociation at interfaces between discotic liquid crystals: The surprising role of column mismatch. *J. Am. Chem. Soc.* **2014**, *136*, 2911−2920.
(41) Groves, C. Developing understanding of organic photovoltaic devices: kinetic Monte Carlo models of geminate and non-geminate recombination, charge transport and charge extraction. *Energy Environ. Sci.* **2013**, *6*, 3202−3217.
(42) Casalegno, M.; Raos, G.; Po, R. Methodological assessment of kinetic Monte Carlo simulations of organic photovoltaic devices: The treatment of electrostatic interactions. *J. Chem. Phys.* **2010**, *132*, 94705.
(43) Casalegno, M.; Bernardi, A.; Raos, G. Numerical simulation of photocurrent generation in bilayer organic solar cells: Comparison of master equation and kinetic Monte Carlo approaches. *J. Chem. Phys.* **2013**, *139*, 024706.
(44) Arkhipov, V. I.; Heremans, P.; Bässler, H. Why is exciton dissociation so efficient at the interface between a conjugated polymer and an electron acceptor ? *Appl. Phys. Lett.* **2003**, *82*, 4605−4607.
(45) Raos, G.; Casalegno, M.; Idé, J. An effective two-orbital quantum chemical model for organic photovoltaic materials. *J. Chem. Theory Comput.* **2014**, *10*, 364−372.
(46) Troisi, A. How quasi-free holes and electrons are generated in organic photovoltaic interfaces. *Faraday Discuss.* **2013**, *163*, 377−392.
(47) Bittner, E. R.; Silva, C. Noise-induced quantum coherence drives photo-carrier generation dynamics at polymeric semiconductor heterojunctions. *Nat. Commun.* **2014**, *5*, 3119.
(48) Ono, S.; Ohno, K. Combined impact of entropy and carrier delocalization on charge transfer exciton dissociation at the donor-acceptor interface. *Phys. Rev. B: Condens. Matter Mater. Phys.* **2016**, *94*, 075305.
(49) Savoie, B. M.; Jackson, N. E.; Chen, L. X.; Marks, T. J.; Ratner, M. A. Mesoscopic features of charge generation in organic semiconductors. *Acc. Chem. Res.* **2014**, *47*, 3385−3394.
(50) Lipparini, F.; Mennucci, B. Perspective: Polarizable continuum models for quantum-mechanical descriptions. *J. Chem. Phys.* **2017**, *144*, 160901.
(51) Liu, T.; Troisi, A. What makes fullerene acceptors special as electron acceptors in organic solar cells and how to replace them. *Adv. Mater.* **2013**, *25*, 1038−1041.
(52) Idé, J.; Fazzi, D.; Casalegno, M.; Meille, S. V.; Raos, G. Electron transport in crystalline PCBM-like fullerene derivatives: a comparative computational study. *J. Mater. Chem. C* **2014**, *2*, 7313−7325.
(53) Troisi, A. Charge transport in high mobility molecular semiconductors: classical models and new theories. *Chem. Soc. Rev.* **2011**, *40*, 2347−2358.
(54) Shuai, Z.; Geng, H.; Xu, W.; Liao, Y.; André, J.-M. From charge transport parameters to charge mobility in organic semiconductors through multiscale simulation. *Chem. Soc. Rev.* **2014**, *43*, 2662−2679.
(55) Yang, H.; Gajdos, F.; Blumberger, J. Intermolecular charge transfer parameters, electron-phonon couplings, and the validity of polaron hopping models in organic semiconducting crystals: rubrene, pentacene, and C_{60}. *J. Phys. Chem. C* **2017**, *121*, 7689−7696.
(56) McWeeny, R. *Methods of Molecular Quantum Mechanics*; Academic Press: London, 1989.
(57) Schatz, G. C.; Ratner, M. *Quantum Mechanics in Chemistry*; Dover Publications: New York, 2002.
(58) Dreuw, A.; Head-Gordon, M. Single-reference ab initio methods for the calculation of excited states of large molecules. *Chem. Rev.* **2005**, *105*, 4009−4037.

DOI: 10.1021/acs.jpcc.7b03640
J. Phys. Chem. C 2017, 121, 16693−16701

(59) Bartlett, R. J.; Musial, M. Coupled-cluster theory in quantum chemistry. *Rev. Mod. Phys.* **2007**, *79*, 291−352.
(60) Piecuch, P.; Kucharski, S. A.; Kowalski, K.; Musial, M. Efficient computer implementation of the renormalized coupled-cluster methods: The R-CCSD[T], R-CCSD(T), CR-CCSD[T], and CR-CCSD(T) approaches. *Comput. Phys. Commun.* **2002**, *149*, 71−96.
(61) Kowalski, K.; Piecuch, P. New coupled-cluster methods with singles, doubles, and noniterative triples for high accuracy calculations of excited electronic states. *J. Chem. Phys.* **2004**, *120*, 1715−1738.
(62) Schmidt, M. W.; Baldridge, K. K.; Boatz, J. A.; Elbert, S. T.; Gordon, M. S.; Jensen, J. H.; Koseki, S.; Matsunaga, N.; Nguyen, K. A.; Su, S.; Windus, T. L.; Dupuis, M.; Montgomery, J. A. General atomic and molecular electronic structure system. *J. Comput. Chem.* **1993**, *14*, 1347−1363.
(63) Vandewal, K.; Benduhn, J.; Schellhammer, K. S.; Vangerven, T.; Rückert, J. E.; Piersimoni, F.; Scholz, R.; Zeika, O.; Fan, Y.; Barlow, S.; Neher, D.; Marder, S. R.; Manca, J.; Spoltore, D.; Cuniberti, G.; Ortmann, F. Absorption tails of donor:C_{60} blends provide insight into thermally activated charge-transfer processes and polaron relaxation. *J. Am. Chem. Soc.* **2017**, *139*, 1699−1704.
(64) Zhou, W.; Xie, S.; Qian, S.; Zhou, T.; Zhao, R.; Wang, G. Optical absorption spectra of C_{70} thin films. *J. Appl. Phys.* **1996**, *80*, 459−463.
(65) Faltermeier, D.; Gompf, B.; Dressel, M.; Tripathi, A. K.; Pflaum, J. Optical properties of pentacene thin films and single crystals. *Phys. Rev. B: Condens. Matter Mater. Phys.* **2006**, *74*, 1−6.
(66) Levy, M. Universal variational functionals of electron densities, first-order density matrices, and natural spin-orbitals and solution of the *v*-representability problem. *Proc. Natl. Acad. Sci. U. S. A.* **1979**, *76*, 6062−6065.

DOI: 10.1021/acs.jpcc.7b03640
J. Phys. Chem. C 2017, 121, 16693−16701